

Calculation of electron-impact 4^1P excitation of calcium

D V Fursa and I Bray

ARC Centre for Antimatter-Matter Studies, Institute of Theoretical Physics, Curtin University of Technology, GPO Box U1987 Perth, WA 6845, Australia

Received 29 April 2008, in final form 17 June 2008

Published 4 July 2008

Online at stacks.iop.org/JPhysB/41/145206

Abstract

The convergent close-coupling method is applied to the calculation of 10 to 55 eV electron-impact 4^1P excitation of the calcium ground state. The results are compared with experiment and other theories. Though the overall agreement may be considered satisfactory there are some minor outstanding discrepancies that would benefit from further consideration, both theoretically and experimentally.

(Some figures in this article are in colour only in the electronic version)

1. Introduction

In his seminal paper Bederson (1969) introduced the concept of a perfect scattering experiment, one which determined the maximum possible information about the collision process. To date there are very few target systems for which this goal has been achieved. One of them is helium and another is calcium. Taking the electron-impact 1P excitation from the ground state as an example, a perfect scattering experiment determines all four of the independent parameters at each scattering angle, which fully test the two collision-frame ($m = 0, 1$) calculated (complex) non-relativistic probability amplitudes. There are several ways to parametrize the scattering information. Typically, the differential cross section $d\sigma/d\Omega$ is used together with the three Stokes parameters P_1, P_2 and P_3 , or the three charge-cloud orientation parameters P_ℓ, γ and L_\perp (Andersen *et al* 1988).

One advantage of Ca over He is that the superelastic technique may be utilized using optical pumping instead of using techniques involving the measurement of the photon polarization in coincidence with detection of an electron. The latter is much slower and the data typically have large error bars at all scattering angles. So long as a suitable laser is available for the transition of interest, the former is much faster at yielding excellent statistics.

From the theoretical standpoint, over the last decade there has been considerable progress in the description of electron-atom collisions at intermediate energies. The convergent close-coupling (CCC) method (Bray and Stelbovics 1992) was developed in response to the long-standing discrepancies between theory and experiment for electron-impact $2p$

excitation of atomic hydrogen. Though these discrepancies proved to be primarily due to experimental issues (Yalim *et al* 1997, O'Neill *et al* 1998, Williams and Mikosza 2006), the CCC method proved to be very successful due to its capacity to treat the target continuum via a systematic pseudostate representation. This turned out to be important at certain electron energies even for elastic scattering and low-lying state excitation of sodium (Bray 1994) and helium (Fursa and Bray 1995). R -matrix (RM) with pseudostates methods (Bartschat *et al* 1996, Badnell *et al* 1998) should yield much the same results so long as convergence with the pseudostate expansion has been obtained and the structure treatment is much the same. For some targets structure is so difficult that a considerable effort is required for just this aspect of the calculation and the B-spline R -matrix (BSR) method has been developed with this in mind (Zatsarinny and Bartschat 2004), though such methods often do not treat the target continuum to convergence. The exterior complex scaling (ECS) method was initially developed for ionization processes (Rescigno *et al* 1999), but has also been applied very successfully to excitation (Bartlett *et al* 2004, Williams *et al* 2006). Another relatively recent development is the time-dependent close-coupling method which complements the time-independent methods for both excitation and ionization (Colgan *et al* 2001).

Following the recent measurements of e-Ca 4^1P excitation utilizing the superelastic technique (Murray and Cvejanovic 2003, Hussey *et al* 2008) and the relativistic distorted wave (RDW) calculations of Chauhan *et al* (2005), the RM calculations of Kawazoe *et al* (2006), and the BSR calculations of Zatsarinny *et al* (2007), we apply the CCC method to

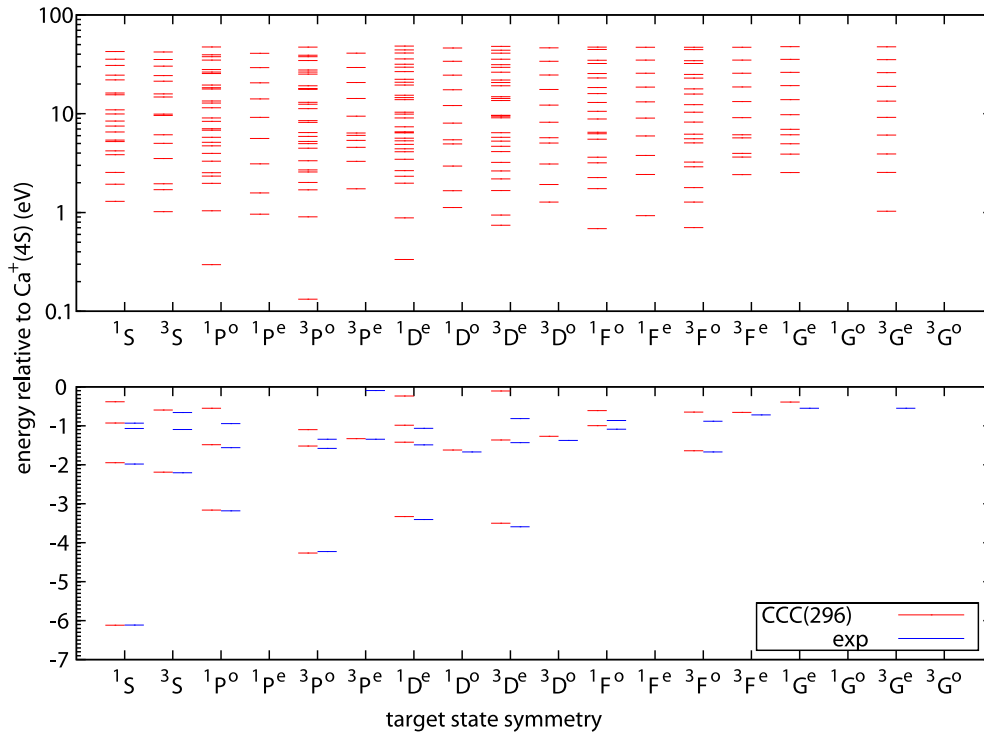


Figure 1. Calcium state energies, relative to $\text{Ca}^+(4S)$ (-11.9 eV), arising in the 296-state CCC calculations. The experimental data are from the NIST database <http://physics.nist.gov/PhysRefData/ASD>.

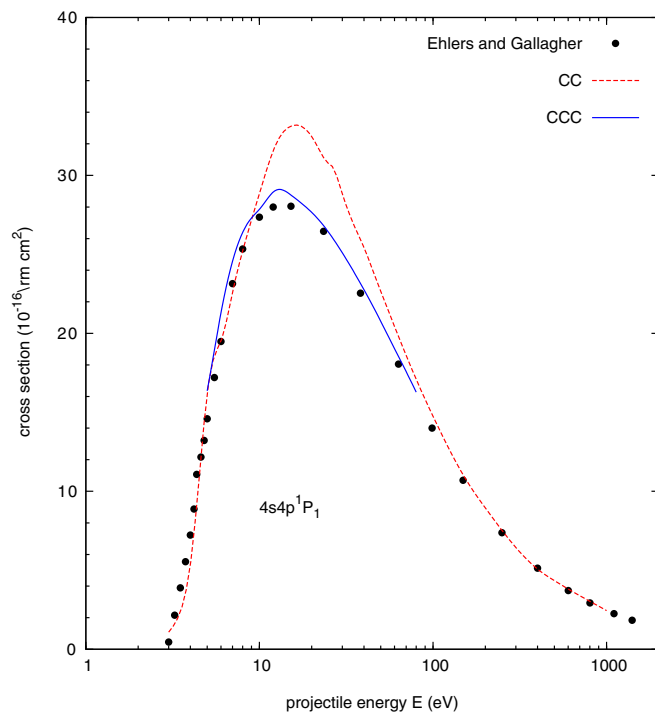


Figure 2. Electron-calcium apparent cross section. The experiment is due to Ehlers and Gallagher (1973). The calculations combine the direct 4^1P excitation cross sections together with cascades from higher excited states. The calculation labelled by CC is convergent in treating only the Ca discrete spectrum, whereas CCC treats both the discrete and the continuous spectrum to convergence.

the problem. The above-mentioned experiments are also complemented by the differential cross sections measurements

of Milisavljevic *et al* (2004), which when taken together (though there is some small energy mismatch) provide the theorists with a complete test of the calculated scattering amplitudes for electron energies ranging from 20 to 55 eV. This is well above the ionization threshold (6.1 eV) and so we expect that neglect of the continuum may have some effect on the results. Given the excellent agreement between the CCC theory and the superelastic measurements of 4^2P excitation in potassium (Stockman *et al* 1998, 1999, 2001) we expect similar agreement in the case of 4^1P excitation of calcium. Our goal is to provide a convergent set of non-relativistic scattering amplitudes for e-Ca 4^1P excitation on a broad energy range, subject only to the frozen-core approximation.

2. Theory

The details of the non-relativistic CCC theory that are relevant to e-Ca scattering have been given by Fursa and Bray (1997). Here we give the essential detail relevant to the present calculations.

2.1. Target structure

The first step is to solve the self-consistent Hartree-Fock equations for Ca^+ to obtain the core-electron wavefunctions. These are then used to define the Ca^+ frozen-core Hartree-Fock Hamiltonian to which a phenomenological core-polarization term is added to obtain accurate Ca^+ wavefunctions. The Ca core polarizability is taken to be 3.26 au. For each l , the resulting Ca^+ Hamiltonian is

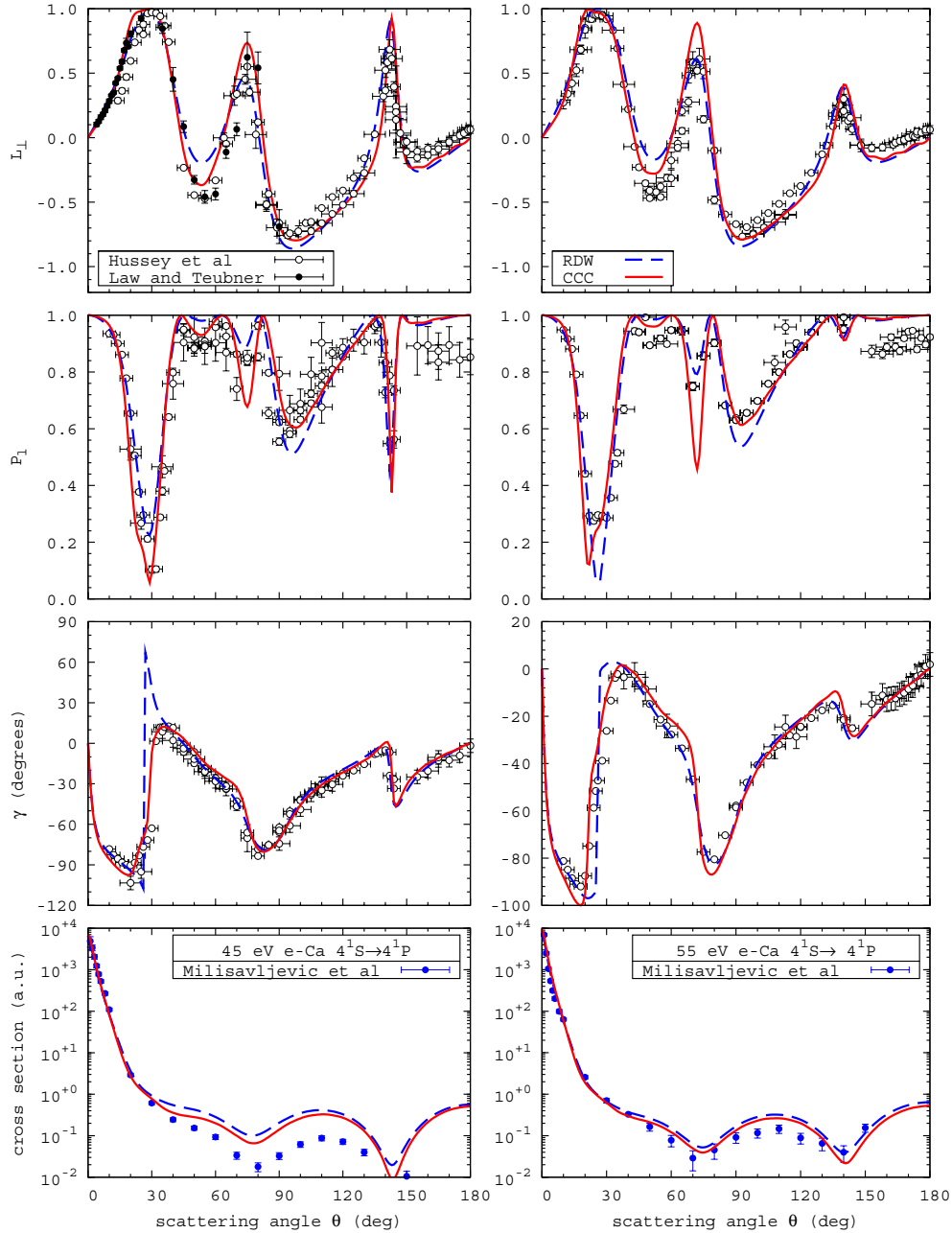


Figure 3. Calcium 4^1P excitation charge cloud orientation parameters and differential cross section for 45 eV (left) and 55 eV (right) electron-impact. The experimental data are due to Hussey *et al* (2008), Law and Teubner (1995) and Milisavljevic *et al* (2004). The latter are presented for the 40 and 60 eV electron energies, respectively.

diagonalized in a one-electron Laguerre basis

$$\xi_{kl}(r) = \left(\frac{\lambda_l (k-1)!}{(2l+1+k)!} \right)^{1/2} (\lambda_l r)^{l+1} \exp(-\lambda_l r/2) L_{k-1}^{2l+2}(\lambda_l r), \quad (1)$$

where the $L_{k-1}^{2l+2}(\lambda_l r)$ are the associated Laguerre polynomials, k ranges from 1 to the basis size N_l , and λ_l is a free parameter. For convenience we take $N_l = N_0 - l$ and $\lambda_l = \lambda$. To simplify the discussion of convergence further we keep $\lambda = 2$ (ideal for 1s of He⁺) leading to just two parameters N_0 and l_{\max} . After diagonalization with a basis size N_l we obtain $n = 1, \dots, N_l$ one-electron orbitals. Typically, the large n orbitals have very high energies and need not be included in subsequent Ca state

calculations. We took $12 - l$ orbitals which give a good span of the discrete and the continuous Ca⁺ spectrum depending on the choice of N_0 . With increasing N_0 the $12 - l$ orbitals move towards the lower energies, thereby emphasizing the discrete spectrum at the expense of the continuum.

Once the Ca⁺ orbitals are obtained they are used to form two-electron configurations, and the Ca frozen-core Hartree–Fock Hamiltonian, together with a phenomenological di-electron polarization potential (Fursa and Bray 1997), is diagonalized to obtain the Ca states. Whereas for helium the two-electron configurations can yield sufficiently accurate states with the ‘inner’ electron being described by the 1s of He⁺ (Fursa and Bray 1995), a more complicated model is required

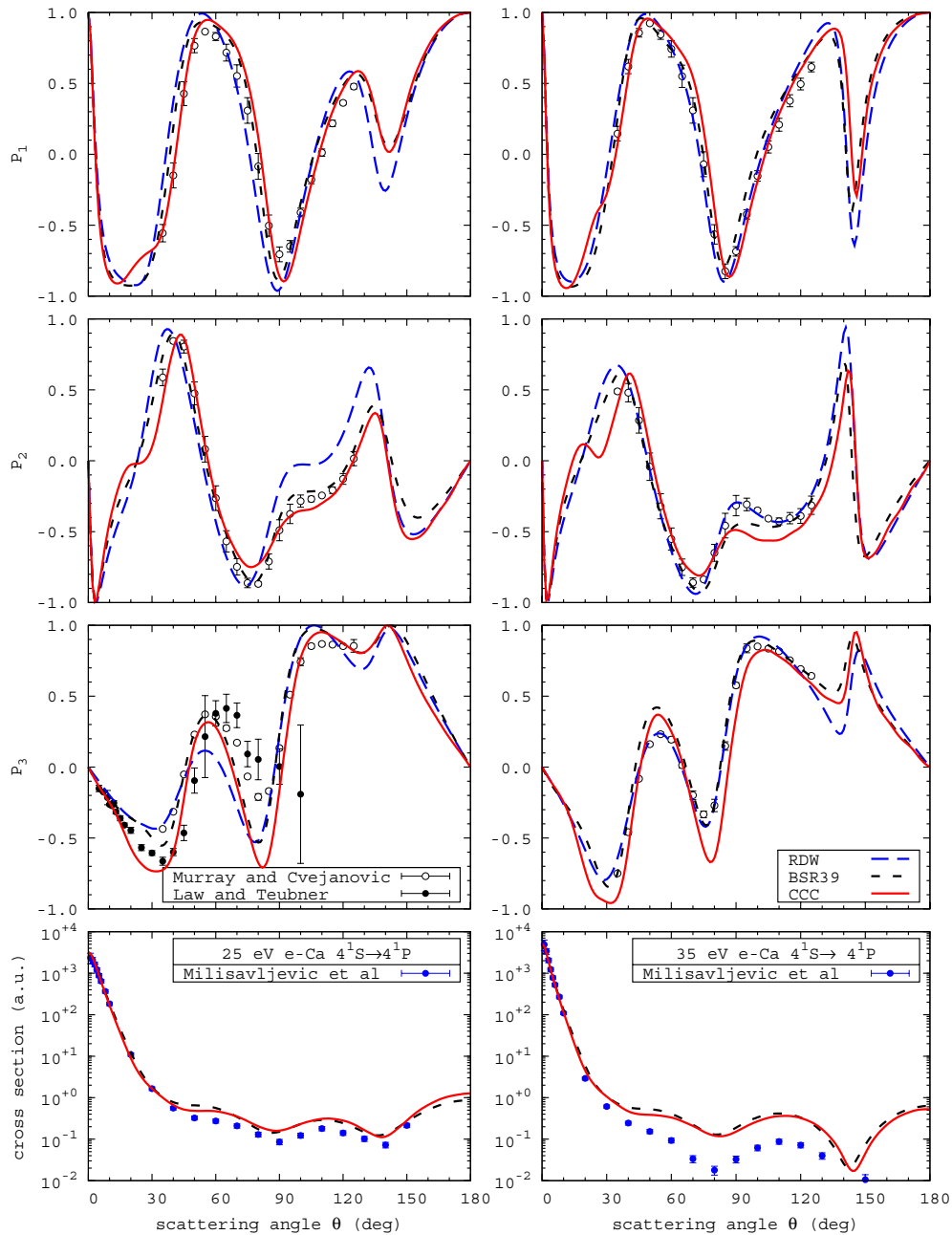


Figure 4. Calcium 4^1P (pseudo) Stokes parameters and differential cross section for 25 eV (left) and 35 eV (right) electron-impact. The experimental data are due to Murray and Cvejanovic (2003), Law and Teubner (1995) and Milisavljevic *et al* (2004). The latter are presented for the 20 and 40 eV electron energies, respectively. The RDW calculations are due to Chauhan *et al* (2005), and the BSR calculations are due to Zatsarinny *et al* (2007).

for the Ca ground and the 4^1P states. Here we combine $\{4s, nl\}$ and $\{4p, nl\}$ configurations that yield accurate higher excited states, with configurations comprising of two lowest lying s-, p-, and d-orbitals. The latter lead to much improved ground and low-lying excited states.

Given the complexity of the target state generation it is important to have a systematic check of the convergence of the electron-scattering calculations. Convergence studies are necessarily dependent on the transition of interest and the projectile energy. Rather than burden the reader with this exercise at each energy we have chosen a sufficiently large calculation that has been checked to have converged to

sufficient accuracy at all energies. This was obtained by taking $N_0 = 20$ and $l \leq l_{\max} = 3$. The resulting 296 state energies are presented in figure 1 and are compared with experiment. We see good agreement for the lowest lying energies, and a very dense discretization of the target continuum.

2.2. Scattering calculations

Having defined the Ca target structure we now proceed to electron-impact calculations. The details of the CCC method for calculating electron scattering on quasi-two-electron targets have been given by Fursa and Bray (1997).

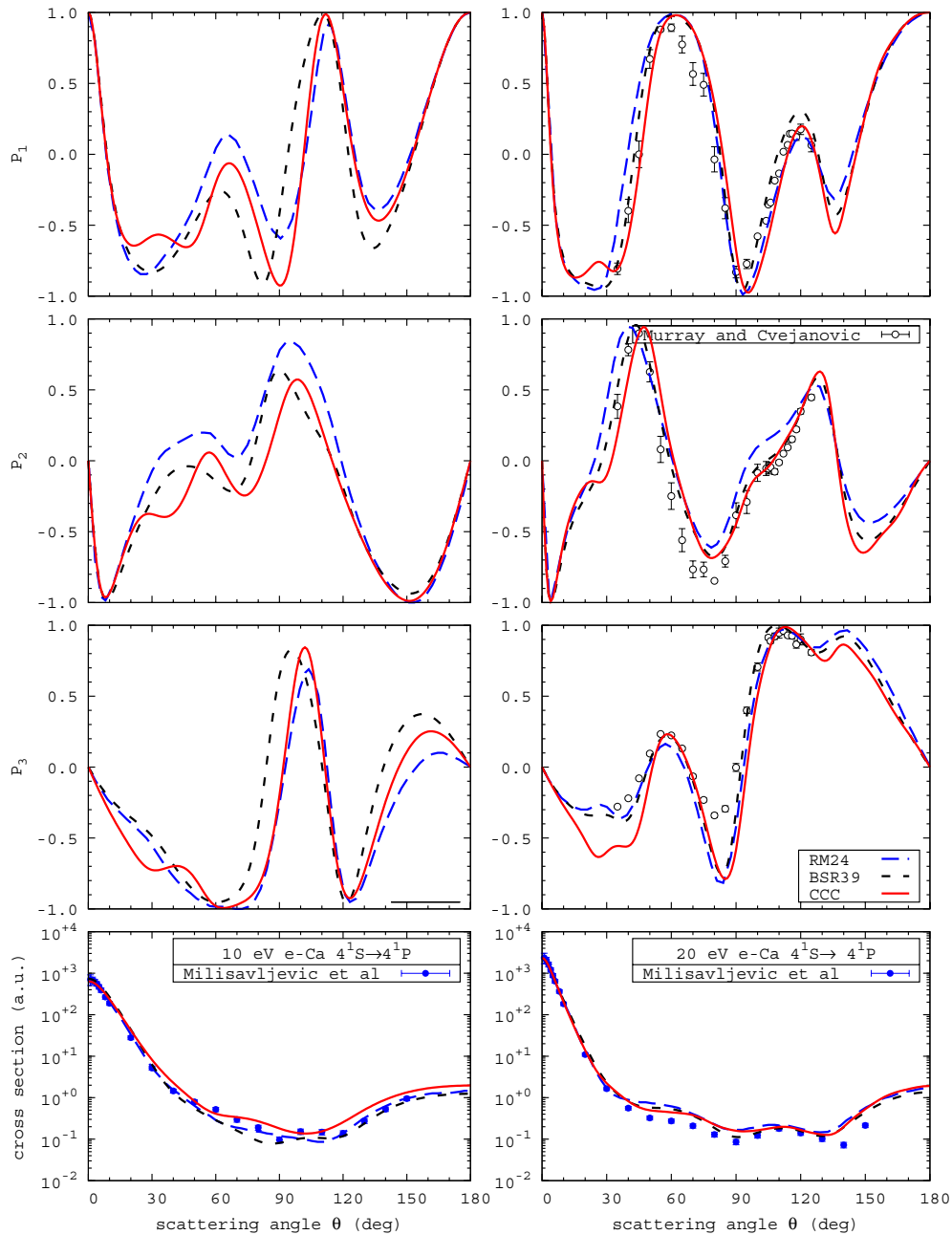


Figure 5. Calcium 4^1P (pseudo) Stokes parameters and differential cross section for 10 eV (left) and 20 eV (right) electron-impact. The experimental data are due to Murray and Cvejanovic (2003) and Milisavljevic *et al* (2004). The BSR calculations are due to Zatsarinny *et al* (2007) and the RM calculations due to Kawazoe *et al* (2006).

Briefly, the Ca target states are used to expand the total wavefunction of the e–Ca system. The close-coupling equations are formulated and solved in momentum space utilizing the partial wave expansion. The strength of the method is that it allows the coupling of a relatively large number of states. This is particularly important when wishing to establish convergence in the treatment of the target discrete and continuous states.

We have already made the point that it is important to treat the target continuum whenever the projectile energy is above the ionization threshold. In figure 2 we demonstrate this by looking at the 4^1P apparent (direct plus cascades) cross section measured by Ehlers and Gallagher (1973). We see the

typical situation where a close-coupling (CC) calculation that neglects the target continuum overestimates the cross section, even for this the largest resonance transition. On the other hand the CCC calculations yield excellent absolute agreement with the experiment.

We next turn our attention to the detailed 4^1P data measured by Law and Teubner (1995), Murray and Cvejanovic (2003) and Hussey *et al* (2008). We begin with the highest incident electron energies for which data are available, namely 45 and 55 eV, presented in figure 3. At these energies we expect perturbative approaches to work well, and indeed the RDW calculation, as well as CCC are generally in very good agreement with the experimental data. Looking in more detail,

the CCC calculations yield slightly better agreement with experiment for the L_{\perp} and P_l minima around 50° . We note that despite the very good agreement at most scattering angles there are some systematic discrepancies with experiment. In particular, at large scattering angles the theories agree with each other, but are well outside the error bars in the case of the L_{\perp} and P_l parameters. Also, at the forward scattering angles both theories are in best agreement with the data of Law and Teubner (1995), published only for L_{\perp} . The full set of data presented by Hussey *et al* (2008) have been plotted, much obtained on an overlapping angular range using the magnetic angle changer (MAC) apparatus. The agreement with some of the data, for example for L_{\perp} around 100° is systematically better than with other data at the same angles. Turning to the differential cross sections, the agreement between the two theories is quite good, though not quite so good with the measurements of Milisavljevic *et al* (2004). We used the same numerical scale for both energies that shows that experiment predicts little variation over this energy range. Hence the observed discrepancies are not due to the 5 eV mismatch in the incident energy.

We next consider the intermediate energies of 25 and 35 eV, presented in figure 4. Here we have additional 39-state B-spline R -matrix (BSR) data of Zatsarinny *et al* (2007) whose bound state structure calculations are of a similar quality to the CCC calculations, but which do not treat the calcium continuum to convergence. Now we start to see occasional considerable variation between the theories. Looking at the P_2 parameter we see that CCC predicts a structure around 30° that is not there in the BSR and RDW theories. It would be interesting if the MAC could be used to study this region. Staying with P_2 , there are some surprising features around 90° . At 25 eV the RDW calculation is considerably above the two other theories and experiment, and yet at 35 eV this is the calculation that best describes the data. Turning to the smaller angles of P_3 we see substantial variation between the three theories around 30° and also variation between the two sets of measurements. This is a somewhat unsatisfactory situation and further experimental and theoretical study could be helpful. The agreement for the differential cross sections is similar to what we saw at the higher energies, good between the theories, but with some discrepancy with experiment at the larger scattering angles.

Lastly, we turn to the consideration of the lowest energies of 10 and 20 eV, presented in figure 5. Here we also compare with a smaller R -matrix calculation of Kawazoe *et al* (2006). While there is good agreement between the calculations and experiment for the differential cross sections, the variation between theories and experiment for the Stokes parameters is quite visible. As at 25 eV for P_3 around 30° , at 20 eV the CCC results lie considerably below the data of Murray and Cvejanovic (2003), whereas the two R -matrix calculations are in quite good agreement here. We have performed many calculations to check the convergence of the presented CCC results and simply note the much better agreement with the data of Law and Teubner (1995) at 25 eV. At 10 eV there is greatest variation between the theories and it would be interesting if subsequent experiment can determine which yield best agreement.

3. Conclusions

We have performed 296-state close-coupling calculations of electron scattering on calcium at a range of energies from 10 to 55 eV. The large size of the calculations is due to the complexity of the target structure and the requirement that the target continuum be treated to convergence at all considered energies. We have concentrated solely on 4^1P excitation with the aim of providing the complete set of experimentally measurable parameters that fully determine the underlying scattering amplitudes. Generally, all of the considered theories give very good agreement with available experiment. Discrepancies are only at the level of detail. In the case of differential cross sections the differences are substantial only where the cross sections are very small. In the case of the Stokes, or the equivalent charge cloud orientation, parameters, only occasionally can notable discrepancies be found. Nevertheless, given the significance associated with the rarely possible complete experimental check of the calculated scattering amplitudes, it would be helpful to revisit the problem at various scattering angles and projectile energies where discrepancies arise. Additionally, it would be helpful to have the differential cross sections (even if relative) determined using the superelastic approach, as has been done in the case of the potassium target (Stockman *et al* 1999).

Acknowledgments

We thank Andrew Murray, Oleg Zatsarinny, Klaus Bartschat, Al Stauffer and Rajesh Srivastava for providing their data in electronic form. This work was supported by the Australian Research Council. We are grateful for access to the Australian Partnership for Advanced Computing and its Western Australian node iVEC.

References

- Andersen N, Gallagher J W and Hertel I V 1988 *Phys. Rep.* **165** 1–188
- Badnell N R, Pindzola M S, Bray I and Griffin D C 1998 *J. Phys. B: At. Mol. Opt. Phys.* **31** 911–24
- Bartlett P L, Stelbovics A T and Bray I 2004 *J. Phys. B: At. Mol. Opt. Phys.* **37** L69
- Bartschat K, Hudson E T, Scott M P, Burke P G and Burke V M 1996 *J. Phys. B: At. Mol. Opt. Phys.* **29** 115–23
- Bederson B 1969 *Comment. At. Mol. Phys.* **1** 41
- Bray I 1994 *Phys. Rev. A* **49** 1066–82
- Bray I and Stelbovics A T 1992 *Phys. Rev. A* **46** 6995–7011
- Chauhan R K, Srivastava R and Stauffer A D 2005 *J. Phys. B: At. Mol. Opt. Phys.* **38** 2385–94
- Colgan J P, Pindzola M S, Mitnik D M, Griffin D C and Bray I 2001 *Phys. Rev. Lett.* **87** 213201
- Ehlers V J and Gallagher A 1973 *Phys. Rev. A* **7** 1573–85
- Fursa D V and Bray I 1995 *Phys. Rev. A* **52** 1279–98
- Fursa D V and Bray I 1997 *J. Phys. B: At. Mol. Opt. Phys.* **30** 5895–913
- Hussey M, Murray A, MacGillivray W and King G 2008 *J. Phys. B: At. Mol. Opt. Phys.* **41** 055202
- Kawazoe S, Kai T, Chauhan R K, Srivastava R and Nakazaki S 2006 *J. Phys. B: At. Mol. Opt. Phys.* **39** 493–503
- Law M R and Teubner P J O 1995 *J. Phys. B: At. Mol. Opt. Phys.* **28** 2257–67

- Milislavljevic S, Sevic D, Pejcev V, Filipovic D M and Marinkovic B P 2004 *J. Phys. B: At. Mol. Opt. Phys.* **37** 3571–81
- Murray A J and Cvejanovic D 2003 *J. Phys. B: At. Mol. Opt. Phys.* **36** 4889–910
- O’Neill R W, van der Burgt P J M, Dzikczek D, Bowe P, Chwirot S and Slevin J A 1998 *Phys. Rev. Lett.* **80** 1630–3
- Rescigno T N, Baertschy M, Isaacs W A and McCurdy C W 1999 *Science* **286** 2474–9
- Stockman K A, Karaganov V, Bray I and Teubner P J O 1998 *J. Phys. B: At. Mol. Opt. Phys.* **31** L867–72
- Stockman K A, Karaganov V, Bray I and Teubner P J O 1999 *J. Phys. B: At. Mol. Opt. Phys.* **32** 3003–13
- Stockman K A, Karaganov V, Bray I and Teubner P J O 2001 *J. Phys. B: At. Mol. Opt. Phys.* **34** 1105–14
- Williams J F, Bartlett P L, Bray I, Stelbovics A T and Mikosza A G 2006 *J. Phys. B: At. Mol. Opt. Phys.* **39** 719–28
- Williams J F and Mikosza A G 2006 *J. Phys. B: At. Mol. Opt. Phys.* **39** 4113–22
- Yalim H, Cvejanovic D and Crowe A 1997 *Phys. Rev. Lett.* **79** 2951–4
- Zatsarinny O, Bartschat K, Bandurina L and Gedeon S 2007 *J. Phys. B: At. Mol. Opt. Phys.* **40** 4023–31
- Zatsarinny O and Bartschat K 2004 *J. Phys. B: At. Mol. Opt. Phys.* **37** 2173–89